The role of negative ions in the formation of particles in low-pressure plasmas

Seung J. Choi and Mark J. Kushner
Department of Electrical and Computer Engineering, University of Illinois, 1406 West Green Street, Urbana, Illinois 61801

(Received 25 August 1992; accepted for publication 29 March 1993)

Large particles (tens of nm to tens of μm in diameter) are problematic in low-pressure (<1 Torr) plasma processing (etching, deposition) discharges because they can contaminate the product and can perturb electron transport. Although the source of these particles has been studied by a number of groups, a definitive explanation is still lacking. In this paper, we theoretically investigate the role of negative ions in the formation of large clusters, the precursors to particles, in low-pressure plasmas. We find that the formation of particles requires a critically large cluster. Forming the critically large cluster requires longer residence times in the plasma than is usually possible if clustering involves only neutral particles. We propose that negatively charged intermediates, which are trapped in electropositive plasmas, increase the average residence time of clusters to allow the growth of critically large clusters.

I. INTRODUCTION

Particulate contamination is almost unavoidable in industrial plasmas. Contamination of plasmas by particles 10s nm–10s μm in size has been experimentally observed in a variety of both direct current (dc) and radio frequency (rf) glow discharges.[1–16] Plasma processing reactors, in particular, are routinely contaminated with particles generated by sputtering and gas phase processes. In fact, the ubiquitous generation of "dust" in low-pressure plasmas has motivated researchers to find methods to enhance particle production in plasmas in order to produce macroscopic quantities of ultrahigh-purity powders.[17–20] Although studies of the transport of particles, and observations of the onset of particulate contamination have been made by a number of workers, the source and method of generation of the particles are still largely unknown. Given the large variety of discharge devices and chemistries in which particles are observed, a single process is not likely to explain all of the sources of particles. For example, carbon particles 100s nm to many microns in size with densities in excess of 10^6 cm^{-3} can be produced in dc rare gas sputter discharges.[10] These nucleation processes are clearly different from those in polymerizing fluorocarbon etching discharges.[2] A common feature of these discharges, however, is that they operate at low pressures (<100 mTorr–1 Torr) and the diffusion time for the loss of neutral reactive particles is commensurate with their rates of reaction in the plasma.

In this paper we discuss requirements for particle growth, and the role of negative ions in nucleation of critically large clusters. This discussion uses results from a model for sputter discharges and nucleation. Particle growth in discharges such as silane plasmas, unquestionably has an important chemical component which is specific to that particular system.[21] In this paper we only address the more general issue of nucleation in low-pressure plasmas. In Sec. II, we describe mechanisms for particle growth, and describe our model in Sec. III. We discuss our results for the formation of clusters having many 100s of atoms in Sec. IV. These clusters are precursors to dust particles having sizes of a few nm to 10s μm. We find that production of gas phase particles most likely depends on there being negatively charged clusters which lengthen the average residence time in the plasma of these precursors. We also find that there are critical gas pressures and power depositions required to generate large particles.

II. MECHANISMS FOR PARTICLE GROWTH

There are many sources of the atoms which ultimately form particles in plasma processing discharges. For example, it has been observed that particles only form after 10s of minutes of operation in initially clean etching reactors using Ar/CCl_2F_2 mixtures.[2] The times for gas phase reactions (and gas residence times) are much shorter than these values. This result therefore suggests that the walls or electrodes of the reactor are coated with a polymeric product, and sputtering of those films after they grow to a given thickness are the source of the material for the particles. On the other hand, observations of rapid particle growth when operating above a critical gas pressure and power deposition in silane discharges are evidence that particles can form dominantly by gas phase reactions.[14] Indeed, in the latter experiments, the total inventory of atoms in the particles appeared to be constant once growth of the particles was initiated: only their size and density evolved.[15] Similar observations were made by Yoo and Steinbruchel.[16] They found that critical pressures and powers were required to grow particles in both sputter etching and reactive ion etching discharges. They also observed that once formed, the number of large particles remains constant while their size increases.

Once a sufficient density of critically large clusters are formed in the gas phase, particle growth rapidly follows. In the context of our work, we define the critical cluster size as having been achieved when the probability that a gas phase radical nucleates with the cluster exceeds the prob-

 0021-8979/93/74(2)/853/9/$6.00 © 1993 American Institute of Physics

ability for the radical being lost by diffusion to the walls. Analogously, the critical cluster size is achieved when the rate of growth exceeds the rate of loss by all processes (evaporation, fragmentation, diffusion).[22] An estimate of the critical cluster size can be made from classical nucleation theory. This theory states that the rate coefficient for reactions between particles having i and j atoms scales as[23]

$$k_{ij} \approx k_0 \frac{(i^{1/3}+j^{1/3})^2}{[ij/(i+j)]^{1/2}}. \quad (1)$$

The numerator accounts for the increase in collision cross section with increasing sizes of the reactants since the radius of a cluster scales as $i^{1/3}$, and the collision cross section scales as the square of the sum of the radii. The denominator accounts the change in the thermal speed of interaction as the reduced mass of the pair of reactants changes. Experimental observations of the uniformity and smooth appearance of particles in most discharges suggest that growth of moderately sized particles is dominated by the accretion of atoms or small clusters by larger clusters as opposed to large particles clustering with large particles ($i \gg j$).[16] [Very large (>10 μm) particles are usually agglomerations of smaller particles.] Since even small particles have many thousands of atoms, each cluster must therefore experience many hundreds to thousands of accretion collisions before being lost to the walls.

For purposes of discussion, we will assume that clusters dominantly grow by accreting monomers or much smaller clusters; that is, $i \gg j$. We will also assume that the monomers and smaller clusters diffuse and stick to walls of the chamber with probability s_w while they stick to a growing cluster with probability s_p. A critical cluster size having n atoms is achieved when the time to nucleate n atoms is shorter than the average time in which those particles are lost to the walls. After this size is reached, particle growth is guaranteed since the rate of growth is larger than the rate of loss by diffusion. This condition is satisfied when

$$\sum_{i=1}^{n} \frac{1}{N_1 k_{1i} s_p} \ll \frac{1}{(D_n/\Lambda^2)s_w}, \quad (2)$$

where N_1 is the density of the accreting monomer vapor, D_n is the diffusion coefficient of a cluster having n atoms, and Λ is the diffusion length of the reactor. The first term represents the time to have the n collisions required to form the cluster; the second term represents the time in which the cluster is lost by diffusion. Since D_n is inversely proportional to gas pressure P, one can show that the scaling parameter of interest which describes formation of the critical cluster is $\gamma = s_p P N_1 k_{1i}/s_w$. This scaling parameter implies that at large gas pressures and low wall sticking coefficients, the critical cluster size is small because the rate of loss by diffusion is small. Similarly, if the density of the monomer vapor is high and the rate coefficient for gas phase reactions is large, the critical cluster size is also small because accretion is rapid.

An estimate of the critical cluster size can be obtained by finding the smallest cluster (above $n=10$) for which Eq. (2) is satisfied. Assuming $s_p/s_w = 1$, and using conditions typical of plasma deposition of a-Si:H ($\Lambda \simeq 1$ cm, gas mixture Ar/SiH_4), the critical cluster size is plotted in Fig. 1 as a function of PN_1k_{1i}. (A discussion of D_n appears in Sec. III.) The critical cluster size increases with increasing γ. To rapidly nucleate (that is, have a small critical cluster size), a value of γ of a few hundred is required. This corresponds to $P=1$ Torr, $k_{1i}=1\times10^{-11}$ cm^3 s^{-1}, and $N_1 = 10^{13}$ cm^{-3}. Clearly, conditions in which large amounts of reactive monomers (large N_1 and large k_{1i}) are formed lead to rapid nucleation (which translates to small critical cluster sizes). These conditions are obtained, for example, at high silane densities and high-power deposition where large densities of SiH_n are generated. Nucleation under these conditions would then be consistent with experimental observations.[14,15]

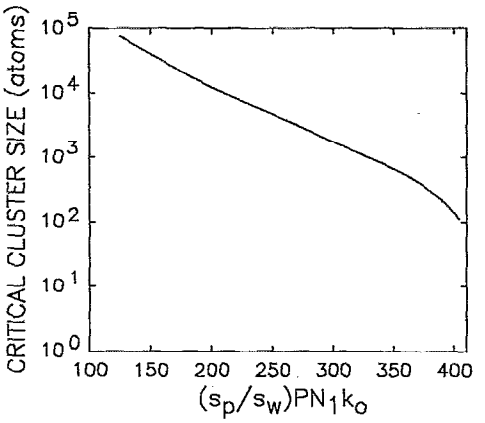

FIG. 1. Critical cluster size as a function of $(s_p/s_w)PN_1k_0$ for neutral clusters. s_p and s_w are the sticking coefficients on other clusters and walls, P is the gas pressure, N_1 is the density of monomer vapor, and k_0 is the collision rate coefficient. Large critical clusters are required at small pressures or monomer density to offset the loss of small clusters by diffusion.

In moderately powered, low-pressure plasmas ($\gamma \ll 100$) the critical cluster size is very large and generating this size cluster before it is fragmented or pumped out of the reactor may be difficult. In order to have rapid particle growth (that is, increase the value of γ), some mechanism must be introduced which lengthens the lifetime of small clusters in the plasma until they reach the critical cluster size.

For purposes of discussion, we will assume that critically, or near critically large, clusters are not sputtered off of electrodes or walls in contact with the plasma but form in the gas phase. Almost by definition, atoms or radicals which form particles must have moderately large reactive sticking coefficients in order to nucleate. It is reasonable, then, to also assume that the electrodes and surfaces in contact with the plasma will be coated with polymerized materials similar to that which is formed in the gas phase. The end result is that the precursor radicals and clusters should react with the walls and electrodes in a similar manner as with the growing clusters. This would mean that $s_p/s_w \approx 1$. Therefore, in polymerizing or reactive plasmas, it is difficult to lengthen the lifetime of clusters in the plasma by assigning a low reactive sticking coefficient on the walls

relative to that with other clusters (that is a large s_p/s_w) to lower the critical size. An exception to this situation is if ions sputter clusters which adhere to the wall, thereby reducing their effective sticking coefficient.

Although the densities of neutral radicals in typical plasma processing reactors greatly exceed those of ions, considerable attention has been paid to the roles of both positive and negative ions in the nucleation process. The definitive works of Reents and Mandich[24,25] have shown that there are many bottlenecks in the nucleation of positive ions in silane plasmas which may prevent large positive ion clusters from forming. They also found, however, that these bottlenecks can be bridged if the silane ion clusters are hydrated by water impurities.[25] Positive ions and positive ion clusters, however, have short residence times in plasmas due to their large ambipolar enhanced rates of diffusion. Their rates of diffusion loss to the walls are typically 10–100 times larger than those for neutral clusters. These observations tend to discount the importance of positive ions in the gas phase nucleation process. The rate coefficients for ion-molecule reactions, however, can exceed 10^{-10} cm^3 s^{-1},[25] which results in there being a moderate flux of small positive ion clusters ($i=2$–4) to the walls and electrodes which may cycle back products to the plasma. This increases the importance of heterogeneous reactions of small clusters on the walls which originate from ion-molecule reactions as compared to the contributions of small clusters originating through a neutral channel.

The source of interest in negative ion based nucleation processes is partly attributed to the observations that large negatively charged particles (>10–100 nm) accumulate near the edges of sheaths in dc and rf discharges.[1–11] A particle 50 nm in radius, though, has $\geqslant 10^6$ atoms, and greatly exceeds the critical cluster size. The fact that these large particles accumulate at the edges of sheaths does require that they be negatively charged. However, their negative charge state is not particularly relevant with respect to the nucleation processes which formed the clusters which preceeded the clusters. Particles of many to 10s nm in size are already much larger than the critical cluster size.

It has, however, been observed that the onset of particle formation can be either eliminated or greatly reduced by operating low-pressure rf plasmas with pulsed or modulated excitation.[26,27] Negative ions, and negatively charged clusters, are virtually trapped in the plasma by the positive plasma potential of the discharges of interest. The only important loss mechanisms for these heavy negatively charged particles are deattachment collisions and ion-ion neutralization. The reduction of the plasma and sheath potentials during the "off" cycle of a modulated discharge allows negatively charged ions and small clusters an opportunity to diffuse to the walls and escape from the plasma. These observations suggest that the clusters which are precursors to large particles may depend upon a negative ion based process to grow to large particles, and these processes may be quite important in determining how critically large clusters form.

As we will discuss below, small negatively charged clusters may be instrumental in the formation of particles in plasmas. The source of those small, negatively charged clusters is, however, problematic. Studies by others have shown that it is common for metal clusters as small as 4–6 atoms to support negative ion states,[28–30] whereas very large clusters charge in the same fashion that a dielectric surface in contact with a plasma negatively charges.[31] Van der Waals clusters of closed shells molecules, such H_2O, will solvate a free electron and negatively charge with cluster sizes as small as 11.[32] The threshold energies for attachment to van der Waals clusters of molecules which have negative electron affinities commonly decrease with increasing cluster size. It has also been experimentally observed that Xe_i^-, $i\geqslant 6$ are stable (possibly extending to as low as $i=2$).[33] Negative ion clusters of Al_i^-, Ag_i^-, and Sn_i^- with $3\leqslant i\leqslant 22$, and Ni_i^- with $3\leqslant i\leqslant 18$ have been observed in laser ablation plasmas, and all have binding energies in excess of 1.5 eV.[34] Given these observations, it is not unusual to expect that small clusters will negatively charge in low-temperature plasmas, be stable in the presence of energetic electrons, and behave similarly to heavy negative ions.

III. DESCRIPTION OF THE MODEL

Nucleation theory in high-pressure gases and plasmas reliably predicts the growth and transport of micron-sized particles.[20,22,35,36] The scaling of that theory to low-pressure discharges, though, is not straightforward because, as discussed above, the residence time of neutral particles in low-pressure plasmas is typically much smaller than the nucleation time. We have developed a model to investigate the formation of small clusters having hundreds of atoms in dc sputter discharge and magnetron plasmas in the context of producing nanocrystalline powders (10s nm),[16–19] and rf discharges in the context of plasma deposition. The purpose of this model is to determine the effect of the charging of negative clusters on nucleation, a process which extends the lifetime of precritical clusters in the plasma. In lieu of such charging the clusters may be lost to the walls before they undergo enough collisions to grow to the experimentally observed sizes.

Nanocrystalline powder formation is typically performed using a dc or rf sputter magnetron source.[16–19] The operating pressure (0.5–1.0 Torr) is significantly higher than that commonly used in sputter deposition discharges. The higher pressure ensures that sputtered atoms are stopped in the gas by collisions, thereby generating a critically dense vapor which leads to gas phase condensation or clustering.

Our model includes electron and ion kinetics, ion-surface sputtering, gas phase transport of energetic sputtered atoms and gas phase nucleation of particles. In this work we have simulated the sputtering and clustering of silicon atoms, though the model is applicable to any material which is similarly sputtered. The species in our model are neutral clusters, negatively charged clusters, the buffer gas (Ar), electrons, and ions.

The model consists of two linked simulations. The first

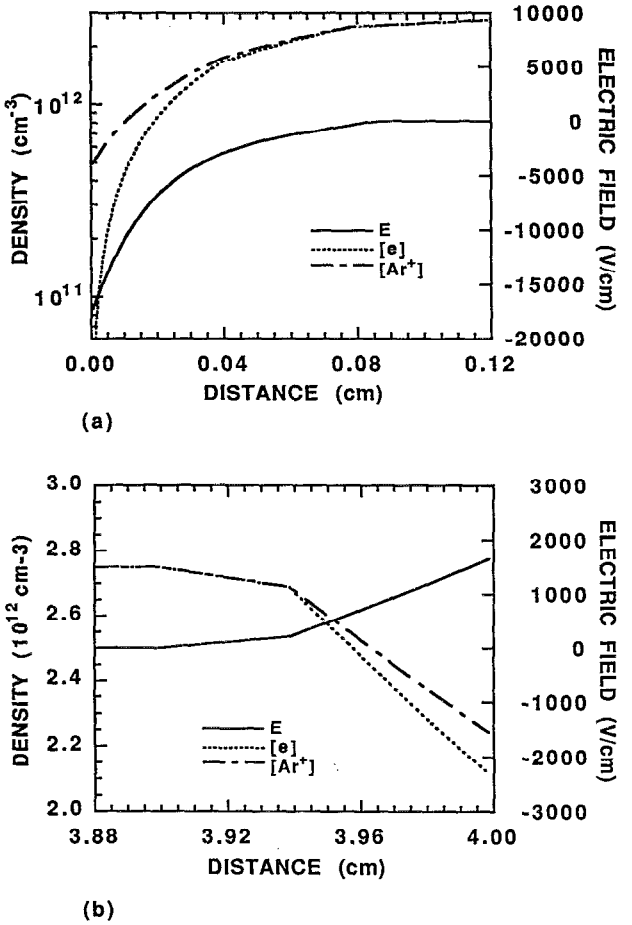

FIG. 2. Typical plasma potential and plasma densities as computed with the beam-bulk discharge model. Quantities are only shown in the vicinity of the (a) cathode and (b) anode.

simulation is a "beam-bulk" model for electron and ion transport in a cathode fall and positive column.[36] In the "beam-bulk" model the electron energy distribution is represented by two components: a monoenergetic beam and a bulk electron swarm. The source of the electron beam is secondary electron emission by ions at the cathode. Continuity equations for the electrons and ions are solved along with Poisson's equation for the electric potential. From this portion of the model, described in more detail in Ref. 37, we obtain the plasma densities and the electric field. The implementation of the discharge model here differs from that in Ref. 37 in that we fully resolve the discharge in one dimension between the cathode and the anode. We also include the reduction in electron mobility resulting from the magnetron fields near the cathode. In doing so, the confining effects of the anode sheath, and the reduction in width and voltage of the cathode fall are accounted for. A typical plasma potential and charged particle densities as a function of position are shown in Fig. 2 for a discharge in 0.6 Torr of argon.

In the second portion of the model, trajectories of energetic sputtered atoms, N_1, are simulated using a Monte Carlo simulation. The source of the sputtered atoms are ion collisions (obtained from the beam-bulk model) with the target cathode. Collisions of sputtered atoms with the buffer gas and with higher-order clusters result in slowing of the sputtered atoms. Monte Carlo algorithms are used to denote whether collisions are elastic or sticking. When the latter occurs the N_1 atom is removed from the simulation. The result of this portion of the simulation is the spatial profile of N_1 atoms in the plasma. The scattering cross section for the collisions was $\pi\sigma_0^2$, where σ_0 is the Lennard–Jones interaction radius.

The effective temperature and mobility of the higher-order clusters are much smaller than the sputtered atoms so a drift-diffusion model is used for the transport of clusters. Given $N_1(x)$ from the Monte Carlo simulation, we solve a set of coupled partial differential equations for the densities of higher-order clusters. The master equation for the density of a cluster having i atoms, N_i, is

$$\frac{\partial N_i}{\partial t} = \sum_{j=1}^{i-1} \frac{1}{2}(1-\delta_{i,i-j}^{-})N_j N_{i-j} k_{j,i-j,i} - N_i \times \sum_{j=1}^{\infty}(1-\delta_{ij}^{-})N_i k_{i,j,i+j} + (1-2\cdot\delta_{ii}^{-}) \times (k_a n_e N_i - k_n N^+ N_i) - \nabla(-\delta_{ii}^{-} N_i \mu_i \mathbf{E} - D_i \nabla N_i) . \quad (3)$$

In the master equation, k_{ijl} (cm^3 s^{-1}) is the rate coefficient for formation of a cluster with l atoms by collision with clusters having i and j atoms; k_a and k_n are the rate coefficients for electron attachment and neutralization; $\delta_{ij}^{-}=1$ when clusters i and j are both charged and zero; otherwise, μ_i^{-} is the mobility of the charged species i; D_i is the diffusion coefficient of a cluster with i atoms; and E is the electric field from the beam bulk model. The terms in Eq. (3) are for homogeneous nucleation, cluster charging and neutralization, and transport.

That portion of the master equation for homogeneous nucleation has been addressed by others in the context of the formation of aerosols, deposition of films, and small scale thermodynamics.[21,22,35,36,38] We additionally consider the transport of the clusters and their charge state. Due to their Coulomb repulsion, charged clusters can only elastically collide with other charged clusters. Clustering reactions therefore occur only on a neutral-neutral or neutral-charged cluster basis. The functional form for the rate coefficients k_{ijl}, which depends upon particle size and mass, is taken from standard nucleation theory and is shown in Eq. (1).[23] k_0 is functionally a parameter in the model from which other rate coefficients are scaled. Since the low pressures of interest may be in the fall-off regime for association reactions, clustering reactions are included as three-body processes using an effective two-body rate coefficient which depends upon pressure.

Directly integrating the master equations for clusters having up to hundreds of atoms as a function of position (10s–100s mesh points) is computationally taxing. The method we used instead is an iterative technique. The master equation for a given cluster can be expressed in matrix form by assuming that the densities of all other clusters are

known or specified. The master equation for each cluster i has the form

$$M^i_{lj}N^i_j=-S^i_j, \tag{4}$$

where N^i_j is the density of cluster i at location j, S^i_j is the source term comprising the first three terms on the right-hand side of Eq. (3), and M^i_{lj} is the transport matrix. Its elements are, in cartesian coordinates,

$$\begin{aligned} M^i_{j-1,j}&=D_i/\Delta x^2-\delta^-_{il}\mu_i E_{j-1/2}/2\Delta x\,,\\ M^i_{jj}&=-2D_i/\Delta x^2-\delta^-_{il}\mu_i(E_{j+1/2}-E_{j-1/2})/2\Delta x\,,\\ M^i_{j+1,j}&=D_i/\Delta x^2+\delta^-_{il}\mu_i E_{j+1/2}/2\Delta x\,, \end{aligned} \tag{5}$$

where Δx is the mesh spacing. In this fashion, $N_i(x)$ can be solved from its master equation by a matrix inversion, $N^i_j=-[M^i_{lj}]^{-1}S^i_j$. This procedure is sequentially performed starting with $i=2$ and progressing to the maximum cluster size of interest. The most recent values of the densities of smaller clusters are used in the kinetic terms of Eq. (3) when forming and solving the master equation of larger clusters. This sequential solution of the master equations (starting at $i=2$ and sweeping through the clusters to higher values) is repeated as many times as required until the distribution converges to a steady state, or the onset of runaway growth is observed. (Typically 100s of sweeps are required.) $N_1(x)$ is then updated by rerunning the Monte Carlo simulation as necessary to reflect changes in $N_i(x)$ $(i>1)$. Conceptually, each sweep through the cluster master equations represents an integration step forward in time since densities of higher-order clusters are obtained in successive sweeps through the master equations. This method either converges to a steady state value or produces a larger density of higher-order clusters with each sweep through the master equations, which indicates that runaway growth has occurred. Although no specific time scale can be assigned to each sweep, we will present our results as sweeps occurring successively in time.

Since the plasma in typical sputter discharges is electropositive, negatively charged clusters are virtually trapped in the plasma. This trapping results in longer average residence times for all particles since the small negative particles are continually being neutralized and ionized in the plasma. As discussed above, studies by others have shown that it is common for small clusters to negatively charge. Due to Coulomb fragmentation, though, small clusters can usually support only a single charge.[39] Van der Waals clusters are weaker in this regard than molecular clusters which may support multiple charges with only tens of atoms.[39] Since the charging mechanisms of large clusters are poorly known, the number of allowed charges per cluster could be considered a parameter in the model. To simplify the calculation, we specified that clusters having less than hundreds of atoms can support only a single charge.

If charged clusters support only a single charge, to first order they appear to be massively large negative ions. A given cluster may sequentially charge by collisions with electrons and be neutralized by collisions with positive ions many times. This cycle of charging and neutralization effectively extends the average lifetime of all clusters in the plasma in spite of the actual steady state density of negatively charged clusters being rather small. In our simulation, we have simply specified that clusters greater than a given size can attach an electron, and parametrized the threshold cluster size for charging.

Diffusion coefficients for the clusters were determined using standard kinetic theory as described in Ref. 40. These coefficients were obtained assuming binary diffusion through the argon buffer gas and using Lennard–Jones potentials. The Lennard–Jones radius for collisions of cluster i with argon was scaled $\sigma_i=(\sigma_{Ar}+\sigma_0 i^{1/3})/2$, where σ_{Ar} is the LJ radius for argon (3.41 Å) and σ_0 was chosen to be that of Si, 2.91 Å.[41] The sticking coefficient on the walls was estimated to be $s_w=0.3$. The attachment rate coefficient was assigned $k_a=5\times10^{-10}$ cm^3 s^{-1} and the ion-ion neutralization rate coefficient was estimated to be $k_n=5\times10^{-7}$ cm^3 s^{-1} (see below).

Association reactions of small clusters typically require third bodies to conserve momentum and stabilize the particle. The rate coefficient for association and clustering processes by different atoms or molecules vary by many orders of magnitude. For example, Gai *et al.* have calculated the rate coefficients for $Si+Si+M\rightarrow Si_2+M$, and for $Si+Si_2\leftrightarrows Si_3$.[42] The effective two-body rate coefficients (at 1 Torr) are 8.5×10^{-18} and 2.4×10^{-18} cm^3 s^{-1}, respectively. These coefficients are small due to the short lifetime of the transition state which, lacking stabilization, decays back to the reactants. It is more likely that small Si atom clusters grow more rapidly by reactions with more than a single Si atom (e.g., $Si_2+Si_3\rightarrow Si_4+Si$), which affords more rapid stabilization.[43]

On the other hand, it is well known that insertion reactions in, for example, silane polymerization are both exothermic and rapid. Guinta *et al.*[44] studied the polymerization process

$$SiH_2+Si_2H_{2n+2}+M\rightarrow Si_{n+1}H_{2(n+1)+2}+M \tag{6}$$

in the context of atmospheric pressure chemical vapor deposition of silicon. They suggested that in the high-pressure limit these reactions have rate coefficients of 4×10^{-11}–2×10^{-10} cm^{-3} s^{-1}. Formation of the smaller silanes at low pressure (1 Torr) is, however, in the fall-off regime and has somewhat lower rate coefficients. For example, Jasinski and Chu[45] measured rate coefficients for SiH_2 insertion into SiH_4 and Si_2H_6. Their values (at 1 Torr) are 6.7×10^{-11} and 1.5×10^{-10} cm^3 s^{-1}, many orders of magnitude larger than those for association reactions of Si atoms.

In our reaction scheme we chose to represent the nucleation chain as a series of third-body stabilized reactions. We parametrized the value of the chain propagating rate coefficient k_0 (as described below) and selected $k_0=10^{-29}$ cm^6 s^{-1} for the presentation of results in this paper. This choice corresponds to an effective two-body rate coefficient divided by s_w of 10^{-12} cm^3 s^{-1} at 1 Torr.

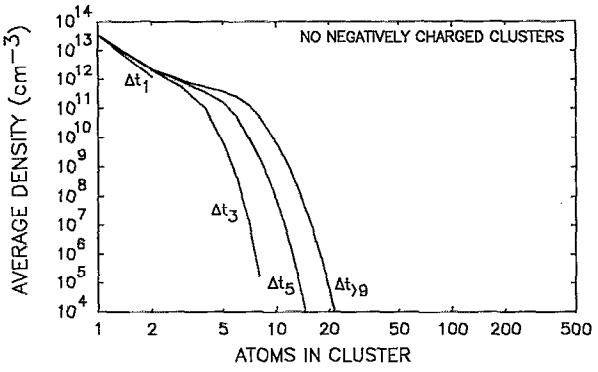

FIG. 3. Predicted densities of higher-order clusters without allowing negatively charged clusters in a sputter discharge as used in formation of nanocrystals. Densities are shown at successive iterations of the master equations, which is conceptually an integration in time.

IV. THE ROLE OF NEGATIVE IONS IN CLUSTERING

A. Sputter sources for nanocrystal formation

Our first study will examine clustering in sputter discharges as used in nanocrystal formation. The discharge conditions were chosen to simulate experimental conditions similar to Hahn and Averback.[17] The Ar buffer gas pressure is 0.6 Torr, cathode current density of 0.4 A cm^{-2}, and chamber size 10 cm. The experimental chamber clearly shows two-dimensional effects with the plasma being confined to a few cm of the target by the confining magnetic field and anode shields surrounding the cathode. While our simulation is one dimensional, we have approximated the experimental conditions by placing a "virtual" anode 4 cm in front of the cathode. The virtual anode collects charged particles as would a real anode, but allows neutral particles to pass through. This effectively confines the plasma near the cathode while allowing neutral chemistry to occur throughout the chamber.

Predicted cluster densities are shown in Fig. 3 when no negative clusters are allowed. Densities are shown for successive iterations through the master equations, which conceptually is an integration in time. When excluding negatively charged clusters, the largest clusters have only 10–15 atoms. Monomer vapor is steadily being produced by sputtering from the target, and is lost to nucleation and diffusion to the walls. A steady-state distribution is nearly obtained after nine sweeps through the master equations. The rate of loss of neutral clusters to the walls is too high to enable the critical cluster size to be achieved.

The density of clusters is shown in Fig. 4 when allowing attachment to clusters having $n \geqslant 5$. On successive sweeps through the master equations, which is conceptually an integration in time, larger clusters are generated. At Δt_{50}, the critical cluster size is reached at $n \simeq 50$–70. At this time, the majority of monomer vapor is consumed by the larger clusters at the expense of clusters having intermediate sizes ($n = 5$–50). At this point, growth is sustained by the accreation of monomers by larger clusters. The clusters of intermediate size are either lost to walls (for lack of monomer vapor to sustain growth) or are consumed by

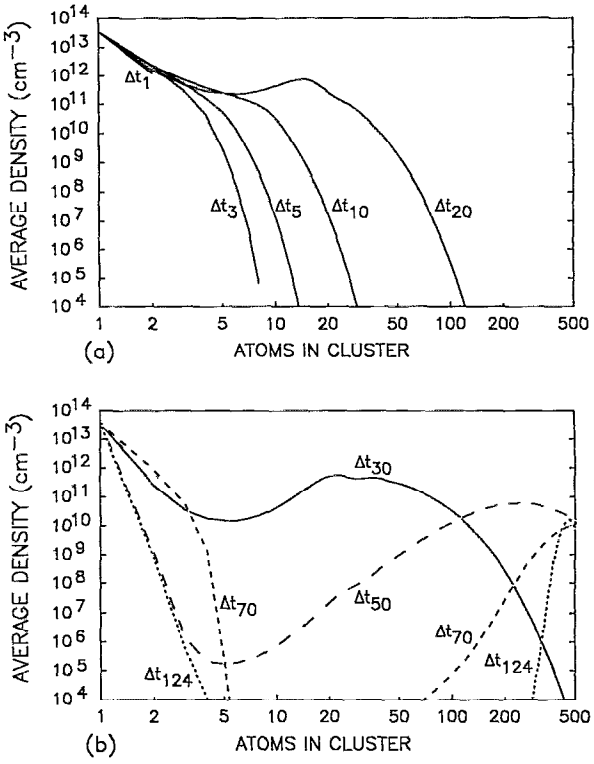

FIG. 4. Predicted densities of higher order clusters while allowing negatively charged clusters ($i \geqslant 5$) in a sputter discharge as used in formation of nanocrystals. Densities are shown at successive iterations of the master equations, which is conceptually an integration in time. A critical cluster size of ~20–50 is indicated.

larger clusters. A peak density near N_{400} is shown after Δt_{124}, which will continue to grow towards larger sizes in a monodisperse fashion. The "breakaway" of a set of large clusters in this fashion is a common feature in high- and low-pressure nucleation having a fixed feedstock of monomers.[15,22] An important difference in these simulations and in most plasma-based nucleation is that there is usually a source of monomer vapor which is continuously sputtered from the target or is produced by electron impact dissociation. This source sustains the nucleation and buoys the density of smaller clusters, which is otherwise consumed by the larger clusters.[15,22] These results also imply that large clusters and small particles should be monodisperse, as experimentally observed.[14–16]

We parametrized the rate coefficients for collisions and sticking coefficients between clusters and on the walls. The effective two-body rate coefficient for nucleation divided by sticking coefficient (k_0/s_w) was parametrized from 1×10^{-10} cm^3 s^{-1} at 1 Torr (corresponding to $k_0 = 10^{-27}$ cm^6 s^{-1}) to 1×10^{-16} cm^3 s^{-1} (corresponding to $k_0 = 10^{-33}$ cm^6 s^{-1}). Nucleation was only obtained for values of $k_0 > 10^{-30}$ cm^6 s^{-1}. We also parametrized the threshold cluster size and rate coefficient for attachment. We were only able to obtain nucleation when attachment began with clusters sizes of $i \leqslant 10$. Nucleation was not observed when $k_a < 10^{-10}$ cm^3 s^{-1}.

The maximum particle size as a function of gas pres-

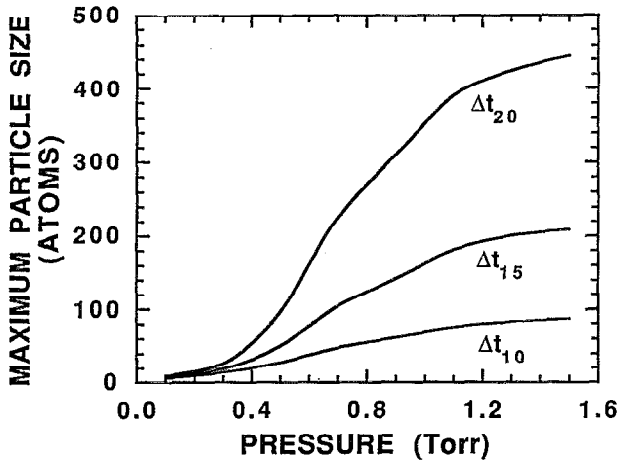

FIG. 5. Maximum size of clusters as a function of gas pressure for the conditions of Fig. 4. Values are shown at various effective times. The maximum cluster size increases with increasing pressure, as a result of lower diffusion losses and higher rates of association reactions.

sure is shown in Fig. 5 at different times after the start of nucleation. The maximum cluster size increases with increasing pressure due to the lower rate of diffusion losses, and the higher rate of association reactions due to three-body enhancement. A critical pressure of 0.2 Torr for nucleation is shown, denoting conditions below which diffusion losses dominate over the rate of nucleation, as experimentally observed.[16] These results, as discussed above, are sensitive functions of the minimum size cluster which we allow to attach. Over a wide range of k_0 and pressure, the minimum cluster which attaches must have $i<10$ even at pressures of ≥ 1 Torr.

The spatial distribution of sputtered monomers (N_1), and neutral and charged clusters having 400 atoms are shown in Fig. 6. The sputtered monomer vapor has a somewhat diffusion dominated profile, while N_{400}^- clusters are confined to the electropositive plasma zone. The density of

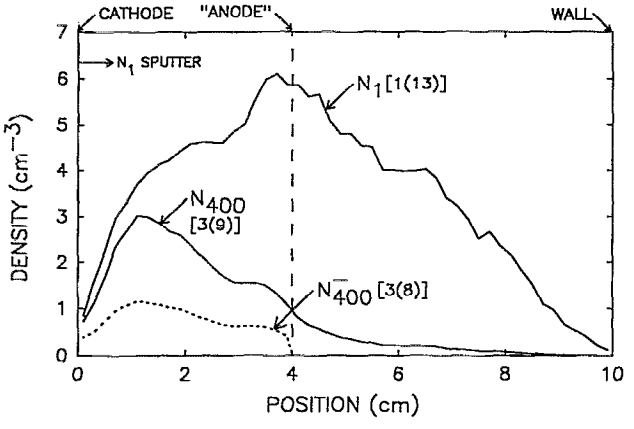

FIG. 6. Spatial distribution of monomer vapor (N_1), and charged and neutral clusters having 400 atoms (N_{400}) in the sputter discharge. The charged clusters are confined to the plasma. The large neutral clusters have a maximum density which also peaks in the plasma.

N_{400} clusters is maximum near the cathode where the clusters intercept the incoming monomer vapor and where the density of the negatively charged clusters is a maximum. The large clusters are then lost by diffusion to the walls of the chamber. Note that only a small fraction of even the large clusters are negatively charged at any given time. In spite of this low density, the cycle of attachment and neutralization effectively lengthens the average lifetime of all clusters in the plasma and accounts for the growth of critically large clusters.

B. rf parallel plate discharges

Particles are often found in low-pressure rf discharges having lower current densities (i.e., lower rate of generation of the monomer vapor) than the sputter discharges modeled above. This result implies that clusters having many atoms may be produced by processes other than accretion from monomer vapor or by having a significant chemical component to cluster growth. These results could also be explained if neutral clusters are essentially nonsticking on surfaces. Sputtering or flaking of large particles from walls or electrodes, or chemical polymerization reactions in the gas phase could provide critically large clusters at low rates of production of monomer vapor. If, however, subcritically large clusters are initially generated, the clusters will most likely have to become charged fairly early in the nucleation process if they are to continue to grow to the critical size.

To demonstrate this effect, we simulated a parallel plate rf discharge (13.56 MHz) in a 200 mTorr gas mixture of $SiH_4/N_2=0.9/0.1$ as used to generate Si_3N_4 particles[46] and to deposit Si_3N_4 films.[47] The electrode separation is 2.54 cm, and the base case power deposition is 25 mW cm^{-2}. A self-consistent Monte-Carlo fluid hybrid simulation for the electron, ion and neutral kinetics was used for this purpose. This model, described in detail in Ref. 48, was used to generate the source of silane radicals by electron impact, electron density, ion densities, and the time averaged electric field as a function of position. These values were then used in the nucleation and clustering model described above to investigate conditions which lead to nucleation in rf deposition discharges. The source of monomer vapor, supplied by sputtering in the calculations discussed above, was replaced by electron impact dissociation of the silane and nitrogen in these examples. As a worst case analysis, we assumed that clustering only proceeded in the manner described above, but with a chemically enhanced rate coefficient, $k_0/s_w=10^{-10}$ cm^3 s^{-1}.

The maximum particle size as a function of power deposition is shown in Fig. 7(a) for various times. The production of monomer vapor in these examples is nearly linearly proportional to the power deposition. A threshold power deposition is predicted at ≈ 60 mW cm^{-2} (or 24 mW cm^{-3}), commensurate with those observed experimentally.[46] This power deposition produces a critical cluster size having ≈ 50 atoms. Powers above this value produce rapid nucleation and growth.

Typical distributions of Si clusters between the electrodes are shown in Fig. 7(b). The neutral clusters have

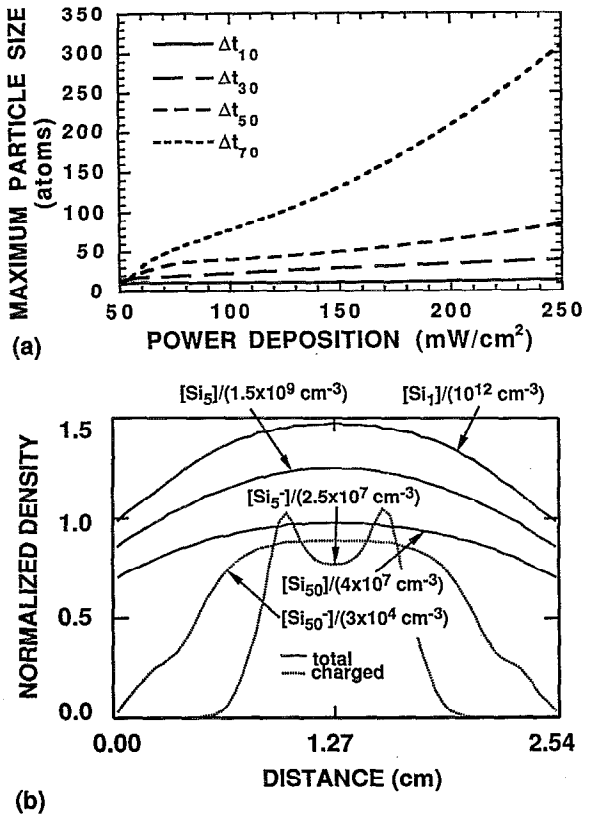

FIG. 7. Characteristics of cluster formation in a parallel plate rf discharge in a NH_3/SiH_4=0.9/0.1 mixture (200 mTorr). (a) Maximum particle size as a function of power deposition. (b) Typical cluster distributions as a function of position between electrodes.

diffusion dominated profiles commensurate with their volumetric sources and sinks at the walls. The negative clusters have a maximum value near the axis at the location where the time-averaged plasma potential is a maximum. Si_6^- has a density which has a local extrema resulting from having sources near the electrodes and sinks in the middle of the plasma.

Recall that large particles accumulate near the edges of the sheaths. Accumulation at this position results from a balance of ion momentum transfer, which pushes particles towards the electrodes, and electrostatic forces which push the particles towards the center of the plasma.[11] The "ion drag" force dominates at low electric fields and for large particle sizes; the electrostatic force dominates at high electric fields and for small particle sizes. Clusters of only a few hundred atoms which support a single charge should therefore accumulate near the maximum of the plasma potential, as shown here, and not at the sheath edges.

V. CONCLUDING REMARKS

We have developed a computer model to investigate the growth of clusters in sputter discharges as precursors to larger particles and nanocrystals. For typical discharge conditions, generating higher-order clusters (> 10s–100s atoms) requires a longer residence time in the plasma than that allowed by neutral diffusion and loss at the walls. Negatively charged clusters, though, are trapped in the electropositive plasma. Our model shows that the longer average residence time afforded by negatively charged clusters allows growth of critically large clusters to occur. The continual cycle of charging and neutralization of small clusters effectively lengthens the life of all clusters even though the instantaneous density of charged clusters may be small. We suggest that clusters as small as 5–20 must be capable of charging negatively in order for this effect to impact rates of nucleation. Applying these algorithms to rf discharges as used in Si_3N_4 deposition shows a threshold power for creating critically large clusters.

Note added in proof. A recently published paper [A. A. Howling, J.-L. Dorier, and Ch. Hollenstein, Appl. Phys. Lett. **62**, 1341 (1993)] reports on experimental measurements of negative ions and particle formation in modulated silane rf discharges. The authors observe a correlation between large negative ion molecules ($Si_n H_m^-$, $n<5$) and the onset of powder formation. They conclude that negative ions are likely precursors to particle formation.

ACKNOWLEDGMENTS

The authors would like to thank R. Averback, C. Steinbruchel, A. Garscadden, G. S. Selwyn, and J. Singh for their insight to nucleation processes in plasmas. This work was sponsored by the Army Research Office (DAAL03-88-K-0094), the National Science Foundation (CTS91-13215, ECS 91-02326), the IBM East Fishkill Facility, the Semiconductor Research Corporation and the University of Wisconsin ERC for Plasma Aided Manufacturing.

[1] G. S. Selwyn, J. E. Heidenreich, and K. L. Haller, Appl. Phys. Lett. **57**, 1876 (1990).
[2] G. S. Selwyn, J. Singh, and R. S. Bennett, J. Vac. Sci. Technol. A **7**, 2758 (1989).
[3] R. M. Roth, K. G. Spears, G. D. Stein, and G. Wong, Appl. Phys. Lett. **46**, 235 (1985).
[4] G. M. Jellum and D. B. Graves, J. Appl. Phys. **67**, 6490 (1990).
[5] K. Spears, T. M. Robinson, and R. Roth, IEEE Trans. Plasma Sci. **PS-14**, 179 (1986).
[6] G. M. Jellum and D. B. Graves, Appl. Phys. Lett. **57**, 2077 (1990).
[7] K. G. Spears, R. P. Kampf, and T. J. Robinson, J. Phys. Chem. **92**, 5297 (1988).
[8] G.S. Selwyn, J. S. McKillop, K. L. Haller, and J. J. Wu, J. Vac. Sci. Technol. A **8**, 1726 (1990).
[9] J. A. O'Neill, J. Singh, and G. S. Gifford, J. Vac. Sci. Technol. A **8**, 1715 (1990).
[10] G. M. Jellum, J. E. Daugherty, and D. B. Graves, J. Appl. Phys. **69**, 6923 (1991).
[11] T. J. Sommerer, M. S. Barnes, J. H. Keller, M. J. McCaughey, and M. J. Kushner, Appl. Phys. Lett. **59**, 638 (1991).
[12] M. S. Barnes, J. H. Keller, J. C. Forster, J. A. O'Neill, and D. K. Coultas, Phys. Rev. Lett. **68**, 313 (1992).
[13] A. Garscadden, "Particles in Plasmas," in Proceedings of the XX International Conference on Phenomena in Ionized Gases, Italy, 1991.
[14] A. Bouchoule, A. Plain, L. Boufendi, J. H. Blondeau, and C. Laure, J. Appl. Phys. **70**, 1991 (1991).
[15] L. Boufendi, A. Plain, J. Ph. Blondeau, A. Bouchoule, C. Laure, and M. Toogood, Appl. Phys. Lett. **60**, 169 (1992).
[16] W. J. Woo and Ch. Steinbruchel, Appl. Phys. Lett. **60**, 1073 (1992).
[17] H. Hahn and R. S. Averback, J. Appl. Phys. **67**, 1113 (1990).
[18] R. S. Averback, H. Hahn, H. J. Höfler, J. C. Logas, and T. C. Shen, Mater. Res. Soc. Symp. Proc. **153**, 3 (1989).
[19] R. Birringer, P. Marquart, H. P. Klein, and H. Gleiter, Phys. Lett. **102A**, 365 (1984).

[20] G. J. Thomas, R. W. Siegel, and J. A. Eastman, Proc. Mater. Res. Soc. **153**, 13 (1989).
[21] In silane plasmas, SiH_2 insertion into saturated silanes (e.g., $SiH_2 + Si_nH_{2n+2} \rightarrow Si_{n+1}H_{2(n+1)+2}$) is an important process for gas phase polymerization. See Refs. 14 and 15.
[22] S. L. Girshick and C. P. Chiu, Plasma Chem. Plasma Proc. **9**, 355 (1989).
[23] J. C. Phillips, Chem. Rev. **86**, 619 (1986).
[24] W. D. Reents and M. L. Mandich, J. Chem. Phys. **96**, 4429 (1992), and references therein.
[25] M. L. Mandich and W. D. Reents, J. Chem. Phys. **96**, 4233 (1992).
[26] Y. Watanabe, M. Shiratani, and H. Makino, Appl. Phys. Lett. **57**, 1616 (1990).
[27] J. T. Verdeyen, J. H. Beberman, and L. J. Overzet, J. Vac. Sci. Technol. A **8**, 1851 (1990).
[28] H. Haberland, in *Fundamental Processes of Atomic Dynamics*, edited by J. S. Birggs, H. Kleinpoppen, and H. O. Lutz (Plenum, New York, 1988).
[29] R. Casero, J. J. Sainz, and J. M. Soler, Phys. Rev. A **37**, 1401 (1988).
[30] O. Echt, in *Proceedings of the 5th Symposium on Atomic and Surface Physics*, edited by F. Howorka, W. Lindinger, and T. D. Mark (Obertraum, Austria, 1986).
[31] M. Mitchner and C. Kruger, *Partially Ionized Gases* (Wiley, New York, 1973).
[32] T. D. Mark, Int. J. Mass Spect. Ion Proc. **107**, 143 (1991).
[33] H. Haberland, T. Kolar, and T. Reineis, Phys. Rev. Lett. **63**, 1219 (1989).
[34] G. Gantefor, M. Gausa, K. -H. Meiwas-Broer, and H. L. Lutz, Faraday Discuss. Chem. Soc. **86**, 197 (1988).
[35] F. S. Lai, S. K. Fiedlander, J. Pich, and G. H. Hidy, J. Colloid Interface Sci. **39**, 395 (1972).
[36] F. Gelbard, Y. Tambour, and J. H. Seinfeld, J. Colloid Interface Sci. **76**, 541 (1980).
[37] S. J. Choi, M. J. McCaughey, T. J. Sommerer, and M. J. Kushner, Appl. Phys. Lett. **59**, 3102 (1991).
[38] G. D. Ulrich, Comb. Sci. Technol. **4**, 47 (1971).
[39] R. Casero, J. J. Saenz, and J. M. Solar, Phys. Rev. A **37**, 1401 (1988).
[40] J. O. Hirschfelder, C. F. Curtiss, and R. B. Bird, *Molecular Theory of Gases and Liquids* (Wiley, New York, 1954), p. 539.
[41] R. A. Svehla, NASA Technical Report R-132, 1962.
[42] H. Gai, D. L. Thompson, and L. M. Raff, J. Chem. Phys. **88**, 156 (1987).
[43] R. D. Kay, L. M. Raff, and D. L. Thompson, J. Chem. Phys. **93**, 6607 (1990).
[44] C. J. Guinta, R. J. McCurdy, J. D. Chapple-Sokol, and R. G. Gordon, J. Appl. Phys. **67**, 1062 (1990).
[45] J. M. Jasinski and J. O. Chu, J. Chem. Phys. **88**, 1678 (1988).
[46] H. M. Anderson, R. Jairath, and J. L. Moche, J. Appl. Phys. **67**, 3999 (1990).
[47] D. L. Smith, A. S. Alimonda, and F. J. von Preissig, J. Vac. Sci. Technol. B **8**, 551 (1990).
[48] T. J. Sommerer and M. J. Kushner, J. Appl. Phys. **71**, 1654 (1992).